

Saturated gain spectrum of VECSELs determined by transient measurement of lasing onset

C. Robin Head,^{1,*} Keith G. Wilcox,² Andrew P. Turnbull,¹ Oliver J. Morris,¹ Edward A. Shaw,¹ and Anne C. Tropper¹

¹*School of Physics and Astronomy, University of Southampton, Southampton, SO17 1BJ, UK*

²*School of Engineering, Physics and Mathematics, University of Dundee, Dundee, DD1 4HN, UK*

*robin.head@soton.ac.uk

Abstract: We describe time-resolved measurements of the evolution of the spectrum of radiation emitted by an optically-pumped continuous-wave InGaAs-GaAs quantum well laser, recorded as lasing builds up from noise to steady state. We extract a fitting parameter corresponding to the gain dispersion of the parabolic spectrum equal to $-79 \pm 30 \text{ fs}^2$ and $-36 \pm 6 \text{ fs}^2$ for a resonant and anti-resonant structure, respectively. Furthermore the recorded evolution of the spectrum allows for the calculation of an effective FWHM gain bandwidth for each structure, of 11 nm and 18 nm, respectively.

©2014 Optical Society of America

OCIS codes: (140.7090) Ultrafast lasers; (140.7260) Vertical cavity surface emitting lasers; (140.3430) Laser theory.

References and links

1. A. C. Tropper, A. H. Quartermann, and K. G. Wilcox, *Advances in Semiconductor Lasers*, (Academic Press, 2012), Chap. 7.
2. U. Keller and A. C. Tropper, "Passively modelocked surface-emitting semiconductor lasers," *Phys. Rep.* **429**(2), 67–120 (2006).
3. K. G. Wilcox, A. C. Tropper, H. E. Beere, D. A. Ritchie, B. Kunert, B. Heinen, and W. Stolz, "4.35 kW peak power femtosecond pulse mode-locked VECSEL for supercontinuum generation," *Opt. Express* **21**(2), 1599–1605 (2013).
4. M. Scheller, T.-L. Wang, B. Kunert, W. Stolz, S. W. Koch, and J. V. Moloney, "Passively modelocked VECSEL emitting 682 fs pulses with 5.1 W of average output power," *Electron. Lett.* **48**(10), 588–589 (2012).
5. K. G. Wilcox, A. H. Quarterman, H. E. Beere, D. A. Ritchie, and A. C. Tropper, "Variable repetition frequency femtosecond-pulse surface emitting semiconductor laser," *Appl. Phys. Lett.* **99**(13), 131107 (2011).
6. O. D. Sieber, V. J. Wittwer, M. Mangold, M. Hoffmann, M. Golling, T. Südmeier, and U. Keller, "Femtosecond VECSEL with tunable multi-gigahertz repetition rate," *Opt. Express* **19**(23), 23538–23543 (2011).
7. C. R. Head, H.-Y. Chan, J. S. Feehan, D. P. Shepherd, S. Alam, A. C. Tropper, J. H. V. Price, and K. G. Wilcox, "Supercontinuum Generation With GHz Repetition Rate Femtosecond-Pulse Fiber-Amplified VECSELs," *IEEE Photon. Technol. Lett.* **25**(5), 1041–1135 (2013).
8. M. C. Stumpf, S. Pekarek, A. E. H. Oehler, T. Südmeier, J. M. Dudley, and U. Keller, "Self-referenceable frequency comb from a 170-fs, 1.5- μm solid-state laser oscillator," *Appl. Phys. B* **99**(3), 401–408 (2010).
9. A. Bartels, D. Heinecke, and S. A. Diddams, "10-GHz self-referenced optical frequency comb," *Science* **326**(5953), 681 (2009).
10. U. Keller, D. A. B. Miller, G. D. Boyd, T. H. Chiu, J. F. Ferguson, and M. T. Asom, "Solid-state low-loss intracavity saturable absorber for Nd:YLF lasers: an antiresonant semiconductor Fabry-Perot saturable absorber," *Opt. Lett.* **17**(7), 505–507 (1992).
11. U. Keller, K. J. Weingarten, F. X. Kärtner, D. Kopf, B. Braun, I. D. Jung, R. Fluck, C. Hönninger, N. Matuschek, and J. Aus der Au, "Semiconductor saturable absorber mirrors (SESAM's) for femtosecond to nanosecond pulse generation in solid-state lasers," *IEEE J. Sel. Top. Quantum Electron.* **2**(3), 435–453 (1996).
12. C. Borgentun, J. Bengtsson, and A. Larsson, "Direct measurement of the spectral reflectance of OP-SDL gain elements under optical pumping," *Opt. Express* **19**(18), 16890–16897 (2011).
13. M. Mangold, V. J. Wittwer, O. D. Sieber, M. Hoffmann, I. L. Krestnikov, D. A. Livshits, M. Golling, T. Südmeier, and U. Keller, "VECSEL gain characterization," *Opt. Express* **20**(4), 4136–4148 (2012).
14. M. E. Barnes, Z. Mihoubi, K. G. Wilcox, A. H. Quarterman, I. Farrer, D. A. Ritchie, A. Garnache, S. Hoogland, V. Apostolopoulos, and A. C. Tropper, "Gain bandwidth characterization of surface-emitting quantum well laser gain structures for femtosecond operation," *Opt. Express* **18**(20), 21330–21341 (2010).

15. C. R. Head, "Optical trapping and optical sources for nanophotonics," Univ. of Southampton, Doctoral Thesis (2013). <http://eprints.soton.ac.uk/359888/>
16. M. Kuznetsov, F. Hakimi, R. Sprague, and A. Mooradian, "Design and characteristics of high-power (>0.5-W CW) diode-pumped vertical-external-cavity surface-emitting semiconductor lasers with circular TEM₀₀ beams," *IEEE J. Sel. Top. Quantum Electron.* **5**(3), 561–573 (1999).

1. Introduction

It has been shown over a long period that vertical-external-cavity surface-emitting semiconductor lasers (VECSELs) readily exhibit stable passive mode-locking under the influence of a semiconductor saturable absorber mirror (SESAM) [1,2]. Only relatively recently, however, have thermal management of the quantum well gain structure, and optical management of the intracavity pulse-shaping process, reached a level at which peak optical pulse powers in the kilowatt regime can be demonstrated [3,4]. The combination of intense femtosecond pulses with broadly tunable GHz repetition rates [5,6] may lend itself to a number of applications such as supercontinuum generation for frequency combs [7–9].

SESAMs [10,11] for these lasers must combine sufficient modulation depth and fast absorption recovery with a high damage threshold, negligible non-saturable loss and sufficiently low dispersion. To define the task for the SESAM, it is important to characterise the gain bandwidth of the VECSEL gain structure, which, together with the photon lifetime of the cavity, defines the amount by which the intracavity pulse is stretched each time it is amplified. Highly sensitive nonlinear reflectivity measurements of gain spectrum and saturation fluence have been reported for VECSEL structures using an external probe laser [12,13]. In these measurements, however, the gain spectrum was determined using a CW tunable laser in the small signal regime. We present a complementary technique, in which the evolution of the gain spectrum can be tracked through the process of gain saturation.

After the onset of lasing the laser spectrum changes in shape over a period of 100 μ s or more. During this process the photon population is slowly redistributed over the cavity modes, out of the wings and into the centre, in response to the spectral curvature of the gain. This slow dynamic narrowing is referred to as spectral condensation.

Barnes et al. [14] employed a spectro-temporal approach to measure the evolution of the laser spectrum in the approach to the steady-state. An acousto-optic modulator (AOM) was used to gate the laser emission onto a spectrometer and thus allowed for the observation of the time-resolved spectral behaviour following the lasing onset. However, due to the response time of the AOM, this spectro-temporal technique had a low time resolution of 4 μ s and was unable to acquire data for very early times, < 18 μ s, after lasing onset.

In this work we present a spectro-temporal technique that enables the observation of the spectral behaviour from within the first microsecond of lasing onset for \sim 100 μ s with a time resolution of 32 ns. The transient spectral information is used to calculate the effective gain bandwidth of the VECSEL gain structures under operating conditions. Furthermore the high time resolution reduces averaging of the spectrum during the recording time window [14], and allows for the calculation of the gain dispersion.

Our VECSEL use resonant periodic gain structures, with optically pumped quantum wells positioned at standing wave antinodes. The thickness of the window layer in the surface-emitting gain structure determines the position of the Fabry-Perot resonance of the active region with respect to the gain wavelength [1]. Two common designs are the resonant and anti-resonant design; where the first enhances the gain at the design wavelength, whereas the latter is designed to have more gain for a broad range of wavelengths around the design wavelength. In this work we demonstrate our technique for both structure designs.

2. Experimental methods

A Z-shaped cavity is used to study the laser build-up characteristics of the gain samples as shown in Fig. 1. A 100-mm radius of curvature (RoC) high reflector (HR) was used to form the short arm of the cavity, whereas the long arm of the cavity consists of a 50-mm RoC HR and output coupler (OC) which were used as a folding mirror and cavity end mirror, respectively. The laser cavity length was about 28 cm. The output coupler had a transmission

of 0.3%. The gain structures were pumped with 1.5 W of power from a fibre-coupled 810-nm diode laser focused to a 60- μm radius pump spot. The gain samples were mounted on a temperature-controlled water-cooled copper heat sink.

The gain samples investigated were 10-quantum-well InGaAs-GaAs VECSEL structures, a detailed description can be found in [3], which were designed by W. Stolz, grown by B. Kunert and processed by B. Heinen at NASP III/V, Marburg. The structures were attached by solid-liquid inter-diffusion bonding onto a diamond heat spreader before chemical etching to remove the substrate. The InGaP cap of the resonant sample was left with its original thickness of $\lambda/2$. The InGaP cap of the second sample was chemically etched to a thickness of $1.25\lambda/4$, a near anti-resonant design. To align the QW emission with the design wavelength the resonant sample and anti-resonant sample were held at 52°C and 20°C respectively. The anti-resonant sample has previously been used to generate pulses with 460-fs duration at 3.3 W of average power [3].

To switch the laser on and off a mechanical chopper was positioned inside the cavity, to unblock and block the cavity mode at the focus in the long arm of the cavity, while maintaining constant pump conditions. The output of the laser was split by a 90:10 beamsplitter (BS), and the small fraction deflected onto a fast photodiode to measure the intra-cavity power build-up behaviour, which was used to trigger the oscilloscope for all subsequent measurements. The remainder of the beam was then directed to a 1-m grating monochromator, with a resolution of 0.3 nm, where it was split into its wavelengths components. A photodiode following the exit slit was used to measure the spectrally-resolved intra-cavity power build-up. A stepper motor was used to step through the wavelengths measured by the photodiode, so that a power build-up measurement was obtained for each wavelength. In order to resolve the transient behaviour we used 1-GHz InGaAs photodetectors and a 200-MHz bandwidth oscilloscope with a risetime of 2.1 ns. The resulting time resolution was 32 ns, limited by digitization by the oscilloscope.

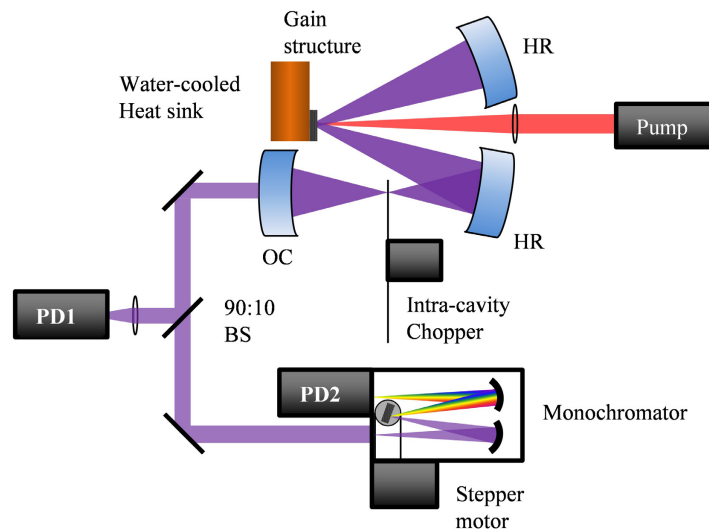


Fig. 1. Schematic diagram of VECSEL and detection system.

3. Results and discussion

The individual spectrally resolved power build-up measurements were recorded for up to 100 μs after lasing onset and then combined into a 2-d data array, Fig. 2(a), coupling the spectral and transient information. The time derivative of each column in the data array, divided by the signal level corresponds to the excess gain over cavity loss in each wavelength channel. Prior

to differentiation the individual traces were binomially smoothed to reduce spikes due to noise or digitization. A mask is applied to ignore intensity values two orders of magnitude lower than the maximum intensity so that dividing by very small numbers is avoided. The net gain was calculated by multiplying the gain per second by the cavity roundtrip time to obtain the net gain per roundtrip. Figure 2(b) shows the net gain spectrum computed in this way and Figs. 2(c) and (d) show the gain spectra at 25 μs and 50 μs , respectively.

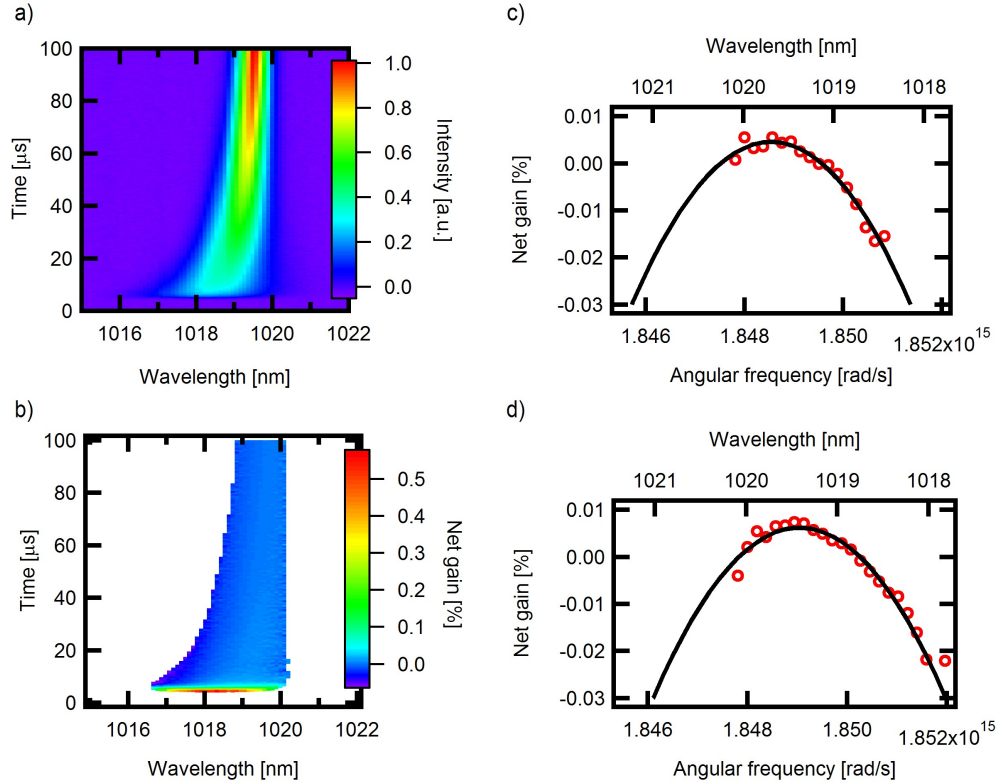


Fig. 2. Spectral evolution, a), and corresponding gain spectrum, b), of the resonant structure. c) & d) are extracted lines of the gain spectrum (red circles) at 25 μs and 50 μs after lasing onset, respectively, including the respective parabolic fits (black line).

The gain spectrum at selected time delays is fitted to the relation $G = B(\omega - \omega_0)^2 + C$ where B is the curvature of the parabola, ω_0 the centre angular frequency and C the offset in the y-direction. Figure 3 shows how each fitting parameter evolves over time. The offset in the y-direction, C , rapidly goes towards zero as the power builds up and the gain saturates [Fig. 3(a)], whereas the curvature, B [Fig. 3(b)], and the centre angular frequency, ω_0 [Fig. 3(c)], of the gain spectrum remain almost constant over the entire time. The initial rise in the curvature of the gain spectrum is thought to be an artefact due to the signal rising above the noise floor. The spikes at later times, past 50 μs , correspond to increased fitting error that arises once spectral condensation has reduced the number of spectral data points. Figure 4 shows the resulting B parameter for the resonant (red) and anti-resonant (black) structure.

The gain dispersion of the VECSEL, $g''(\omega)$, is related to the fit parameter by $g''(\omega) = 2B$. The time-averaged values of B from the data of Fig. 4, excluding early times, correspond to gain dispersion values of $d^2g/d\omega^2 = (-79 \pm 30) \text{ fs}^2$ and $(-36 \pm 6) \text{ fs}^2$ for the resonant structure and anti-resonant structure, respectively. The spectrum of the resonant sample is narrower, so fewer data points are available to fit to in the wavelength dimension, and thus the resulting error is greater.

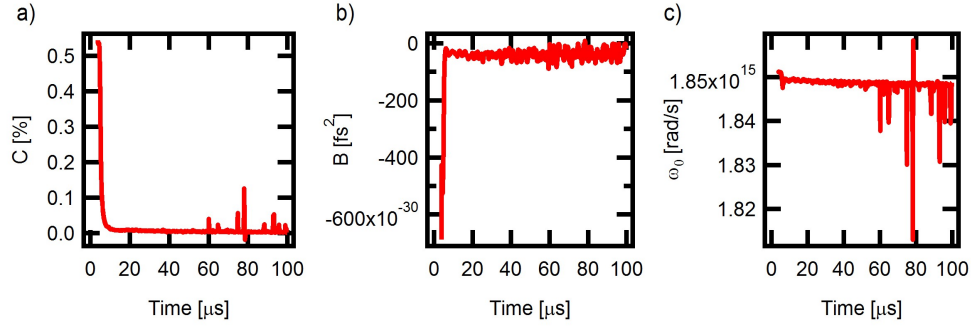


Fig. 3. Evolution of the fit parameters: a) the offset in the y-direction b) curvature of the parabola, and c) the centre angular frequency.

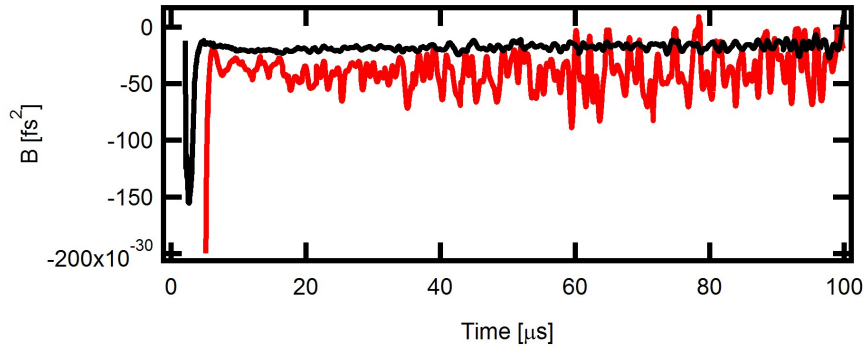


Fig. 4. Evolution of the curvature, B , of the parabolic fits to the gain spectrum for the resonant (red) and anti-resonant (black) structure.

In order to extract an effective half-width half-maximum gain bandwidth, Ωg , for both samples we apply the method described in Barnes et al.'s [14] work based on an analytical model that $\Omega g = (1/(\tau_c dA/dt))$ where τ_c is the cavity photon lifetime. The quantity A is defined by $A = 1/(2\mu_2)$, where μ_2 is the spectral variance of the spectrum at generation time t . The variation of A with time, derived from data as shown in Fig. 2 for the anti-resonant and resonant structures, is plotted in Figs. 5(a) and (b) and exhibits the expected linear evolution. The slope of a straight line fit to the data is used to provide dA/dt .

The cavity photon lifetime, $\tau_c = 0.43 \mu s$, is obtained using a method which involves deconvolution of the photoluminescence (PL) transient from the intra-cavity laser power transient [15]. We use this instead of the Findlay-Clay method, as the Findlay-Clay method assumes that the laser gain transition is represented by a 4-level system, and that the output coupler can be changed with no other effect on cavity alignment, which we believe is unlikely to be true in the case of these low-gain lasers. The transient PL analysis, by contrast, is measured on the identical cavity used for the spectral measurement, and assumes only that spontaneous emission dominates over defect and Auger recombination [16].

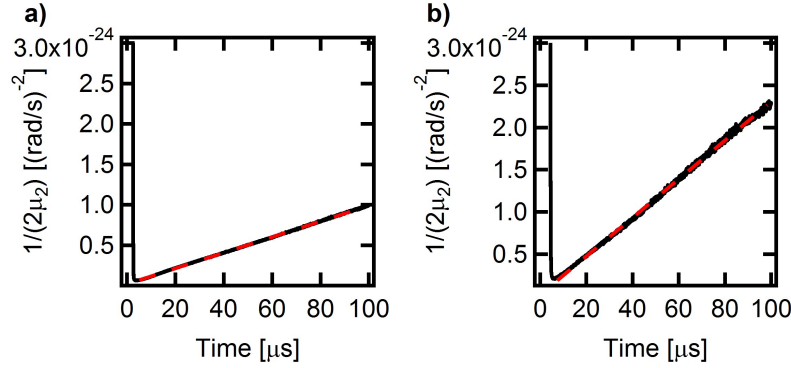


Fig. 5. Evolution of $A = 1/(2\mu_2)$ with generation time for a) the anti-resonant and b) resonant sample. The red (dashed) line is a straight line fit with a slope of 9.72×10^{-21} s/rad² and 2.26×10^{-20} s/rad², respectively.

The calculated values of effective full-width half-maximum (FWHM) gain bandwidth for the resonant structure and the anti-resonant structure are 11 nm and 18 nm, respectively. The FWHM of 18 nm reported here is narrow compared to previously published values of around 30 nm for anti-resonant structures capable of sub-ps pulse duration generation [13,14]. However these experiments were either performed with high pump densities of up to 740 MW/m² or with unprocessed gain structures, raising the active region temperature. The anti-resonant structure studied here has, indeed, been used to generate sub-ps pulses under high power pumping conditions [3]. At higher pump powers an instability appeared preventing the observation of a single smooth transient. The origin of this is still under investigation.

We infer, in this low power pumping experiment (133 MW/m²), that the intrinsic gain bandwidth of the quantum wells, of about 15 nm, was the limiting factor. The filter induced by the longitudinal confinement factor decreased (increased) the overall gain bandwidth for the resonant (anti-resonant) structure measurably, 3-4 nm, but not dramatically. Mode-locked VECSELs appear to generate the shortest pulses when pumped close to rollover to maximise the intrinsic gain bandwidth. Wilcox et al. have described such a laser, with the same gain structures, where the pulse duration decreased with increasing pump power from a 530-fs pulse duration with a pump power density of 325 MW/m² to 400 fs at 630 MW/m² [3].

4. Conclusion

In conclusion we observed that the gain dispersion remained constant as the population inversion saturated in the approach to steady state. The gain dispersion for the investigated structures, a resonant and an anti-resonant structure, were found to be -79 ± 30 fs² and -36 ± 6 fs² with an effective FWHM bandwidth of about 11 and 18 nm, respectively. The relatively small difference between the two samples is attributed to the low intrinsic gain bandwidth of the quantum wells, due to the low pump power used, suggesting that femtosecond pulse durations demonstrated using structures of this type are probably achieved by the broad intrinsic gain profile that develops close to rollover. The presented method and obtained results will not only enable better sample characterisation and design of VECSELs for sub 400-fs pulse durations at multi-watt level average powers, but also allow for the observation of semiconductor laser build-up dynamics in the class-A regime.

Acknowledgments

This work was undertaken with funding from EPSRC (EP/G059268/1). C. R. Head is supported by an EPSRC Doctoral Prize Fellowship and K. G. Wilcox holds an EPSRC Early Career Fellowship.